Available online at www.sciencedirect.com
ScienceDirect
Journal of Non-Crystalline Solids 352 (2006) 3530–3534
JOURNAL OF NON-CRYSTALLINE SOLIDS
www.elsevier.com/locate/jnoncrysol

# Fabrication and characterization of $Er^{3+}$-doped $GeO_2$–PbO and $GeO_2$–PbO–$Bi_2O_3$ glass fibers

L.R.P. Kassab [a,*], W.G. Hora [a], J.R. Martinelli [b], F.F. Sene [b], J. Jakutis [a,c], N.U. Wetter [c]

[a] *Laboratório de Vidros e Datação, Faculdade de Tecnologia de São Paulo, São Paulo-SP, Brazil*
[b] *Centro de Ciência e Tecnologia de Materiais, IPEN-SP, São Paulo-SP, Brazil*
[c] *Centro de Lasers e Aplicações, IPEN-SP, São Paulo-SP, Brazil*

Available online 24 July 2006

**Abstract**

Glass fibers were drawn from $GeO_2$–PbO–$Bi_2O_3$ and $GeO_2$–PbO melts previously doped with $Er^{3+}$. From the differential thermal analysis curve, the glass transition temperature was determined to be 420 °C, and no crystallization peak was observed in the temperature range of that analysis, indicating stability with regard to devitrification. Raman spectroscopy was performed to characterize the structure of the glasses, which exhibited large transmission windows (0.5–5.0 μm) and large refractive indices (~2.0). Infrared to visible upconversion of $Er^{3+}$ was observed in the fibers. The visible emissions were related to the upconverted green emissions at about 530 nm ($^2H_{11/2} \rightarrow {}^4I_{15/2}$) and 550 nm ($^4S_{3/2} \rightarrow {}^4I_{15/2}$), and red emission at 668 nm ($^4F_{9/2} \rightarrow {}^4I_{15/2}$) under 980 nm excitation. The infrared transition ($^4I_{13/2} \rightarrow {}^4I_{15/2}$) was peaked at 1.53 μm. The results obtained suggest that the fibers exhibit the same structures as the parent glasses and can be used in upconversion fiber optical devices.


*PACS:* 42.70.−a

*Keywords:* Optical fibers; Oxide glasses; Germanates; Rare-earths in glasses

## 1. Introduction

Although the glass forming property of germanium dioxide has been known for a long time, the systematic study of germanate glasses and the glassy properties of germanium oxides have only recently begun. Applications include fiber optics, seals for ultra high vacuums, laser media and glasses with specially tailored dispersion properties. Among the heavy metal oxide (HMO) glasses, germanate-based glasses are potential candidates for applications in optical devices because of their low transmission loss in the mid-infrared region [1,2]. Recently these glasses have been drawn into optical fibers due to their good mechanical strength, high thermal stability, good chemical durability and high refractive index (~2) [3]. The heavy metal germanate and the heavy metal fluoride (HMFG) glass fibers are two infrared (IR) transmitting glass fiber systems that are relatively similar to the most popular silica glass fibers. Germanate glass fibers generally do not contain fluoride compounds; instead they contain heavy metal oxides that shift the IR absorption edge to longer wavelengths (~5 μm). The advantage of germanate glass fibers over the HMFG fibers is that germanate glasses usually have better chemical durability, mechanical stability, a higher glass transition temperature and, as a consequence, higher laser damage thresholds at 3 μm. Because of this latter feature, HMOG fibers based on undoped $GeO_2$ glasses have recently shown great promise as an alternative to HMFG fibers for high power laser delivery at the Er:YAG (2.97 μm) wavelength used in many medical and odontological applications [4–6].

* Corresponding author. Tel.: +55 11 55423302; fax: +55 11 33267611.
*E-mail address:* kassablm@osite.com.br (L.R.P. Kassab).

0022-3093/$ - see front matter © 2006 Elsevier B.V. All rights reserved.
doi:10.1016/j.jnoncrysol.2006.03.086

In this paper, the fabrication and characterization of $Er^{3+}$-doped $GeO_2$–PbO and $GeO_2$–PbO–$Bi_2O_3$ fibers for application with optical devices that make use of the upconversion mechanism are reported. There has been increasing interest in rare-earth doped materials for photonic applications such as upconversion (the mechanism that converts low energy photons into visible light) [7–9]. The low phonon energy of germanate glasses (around 700 $cm^{-1}$) compared to borate (around 1400 $cm^{-1}$) and phosphate (around 1200 $cm^{-1}$) glasses [10] indicates (but does not guarantee) low non-radiative relaxation rates, and can make upconversion easily observable compared to oxide glasses that have large multiphonon relaxation rates [11]. Of course, the low phonon energy by itself cannot guarantee a low multiphonon decay since the latter also depends on the electron–phonon coupling with the glass host. However it is a good indication of low non-radiative losses.

Germanate glass fibers were produced using glasses doped with 1.0 wt% of $Er_2O_3$. The compositions of the $GeO_2$–PbO–$Bi_2O_3$ and $GeO_2$–PbO glasses were based on the previous compositions suggested by Balda et al. for $Nd^{3+}$-doped glasses [12].

Results of infrared to visible upconversion of $Er^{3+}$ ions have been presented using $GeO_2$–PbO–$Nb_2O_5$, $GeO_2$–PbO–$CaCO_3$, $GeO_2$–PbO–BaO–ZnO–$K_2O$ and $GeO_2$–PbO–CaO–$TeO_2$ glasses [7–9]. This research group recently reported the upconversion effect in $GeO_2$–PbO–$Bi_2O_3$ glasses; the results obtained motivated the group to produce and characterize $GeO_2$–PbO–$Bi_2O_3$ glass fibers [13]. The spectroscopic properties of $GeO_2$–PbO glasses doped with $Er^{3+}$ have also been presented for applications in the infrared region [14]. In this case, the upconversion effect has not been explored, and also motivated this paper. The aim of this paper is to produce glasses and glass fibers based on two different compositions ($GeO_2$–$Bi_2O_3$ and $GeO_2$–PbO–$Bi_2O_3$ doped with $Er^{3+}$), and to present the results for infrared, upconversion and Raman measurements. A comparison between the fibers and the parent glasses is also performed in order to show that the fibers exhibit the same structure as the parent glasses.

As far as is known, there are no studies that demonstrate the production of $Er^{3+}$ doped $GeO_2$–$Bi_2O_3$ and $GeO_2$–PbO–$Bi_2O_3$ fibers, the infared to visible upconversion effect and the Raman investigation in both systems.

## 2. Experimental procedure

### 2.1. Glass preparation

Glasses were prepared by adding 1.0 wt% of $Er_2O_3$ to the following compositions: $59GeO_2$–41.0PbO (named GP) and $62.5GeO_2$–12.5PbO–25.0 $Bi_2O_3$ (named GPB), in mol%. In each case, mixtures of high-purity (Aldrich 99.999%) raw materials (batches of 15 g) were melted, for 1 h in alumina crucibles at 1050 °C, poured onto a heated brass mold and then annealed at 420 °C, for 3 h. Care was taken during the preparation in order to reduce $OH^-$ contamination. One of the main sources of $OH^-$ impurities can be the starting materials, so the raw materials were treated for 1 h at 300 °C. Glass blocks $(20 \times 20 \times 2)$ $mm^3$ were made to be further used in the fiber-drawing process. Based on energy dispersive spectroscopy (EDS–SEM), the final concentration of the bulk materials were assumed to be identical to the nominal composition used for the batch preparation. By using differential thermal analysis, the glass transition temperature was determined to be 420 °C, and no crystallization peak was observed in the temperature range of that analysis, indicating stability with regard to devitrification.

### 2.2. Fiber fabrication

Fibers were produced from Er-doped germanate glasses using the compositions mentioned above. Cubic pieces of $(20 \times 20 \times 2)$ $mm^3$ were initially grounded in a planetary ball mill (Pulverisette–Fritsch) and melted in an alumina crucible, at 800 °C, for 1 h using a vertical electrical furnace. The temperature was then slowly decreased to 750 °C when the liquid viscosity became appropriate for pulling glass fibers manually. At this temperature the liquid viscosity was within the working range, making the pulling process possible. Fibers were pulled continuously by touching the liquid surface with the tip of a silica rod and moving it upwards using constant speed. Fibers with a diameter of 150 μm and length varying from 1 to 5 m were produced and selected afterwards according to the best uniformity and homogeneity.

### 2.3. Raman spectroscopy

The Raman spectra of the glasses were taken at room temperature coupled to a metallurgical microscope. The spectra were obtained in the 200–1500 $cm^{-1}$ range by exciting the samples at 457.9 nm with an He–Ne laser.

### 2.4. Near infrared and upconversion measurements

The visible and near infrared spectra were measured by pumping the samples optically with a high power diode laser emitting an average power of 5 W at 960 nm (50% duty cycle), dispersing the sample luminescence with a 30 cm monochromator and collecting the signal with a S-20 phot-multiplier. In order to enhance the signal from the small fibers, an imaging system was used that imaged the fibers onto the slit of the monochromator with the exact dimensions of the slit $(0.1 \times 10)$ $mm^2$. Data were analyzed using a lockin amplifier (EGG) coupled to a computer. The spectrum showed a noise level of approximately 5%; this value is estimated by the noise to signal ratio of 1/20.

## 3. Results

In previous studies of GPB glasses performed by this group [13], the incorporation of $Er^{3+}$ was observed in the absorption spectra measured at room temperature, which showed the typical bands of $Er^{3+}$ related to the transitions from the $^4I_{15/2}$ ground state to the excited sates. The same phenomenon was observed for the GP composition but it was not presented in that report. Fig. 1 shows the absorption spectra for GPB and GP glasses doped with 1.0 wt% of $Er_2O_3$.

In the same report [13], it was indicated that the highest emission for infrared transition (peaked at ~1.53 μm) and for upconverted emissions occurred at 1.0 wt% of $Er_2O_3$ in GPB glass. The same behavior was also observed for the GP glass, leading the group to produce the glasses and the glass fibers with this doping level. It is highlighted that the quenching for higher concentrations is attributed to the cross-relaxation mechanism between $Er^{3+}$ pairs, such as $^4I_{13/2} + {}^4I_{13/2} \rightarrow {}^4F_{9/2} + {}^4I_{15/2}$. Fig. 2 shows the emission spectra related to the $^4I_{13/2} \rightarrow {}^4I_{15/2}$ transition (peaked at 1.53 μm) for fibers with GP and GPB compostions. The emission of the GPB glass is also included for comparison. Figs. 3 and 4 show the upconverted emissions (discussed in the next section) for glass fibers and the parent glasses (GPB and GP, respectively). The green luminescences with maxima around 530 nm and 550 nm are assigned to the $^2H_{11/2} \rightarrow {}^4I_{15/2}$ and $^4S_{3/2} \rightarrow {}^4I_{15/2}$ transitions, respectively, and the signal at 668 nm is ascribed to the $^4F_{9/2} \rightarrow {}^4I_{15/2}$ transition. The most intense emission (easily seen by the naked eye) correspond to the green emission from the $^4S_{3/2}$ level. The good agreement between the results indicates the glassy state of the GP and GPB fibers. Furthermore, these emissions are in agreement with previous investigations on erbium-doped glasses [7–9].

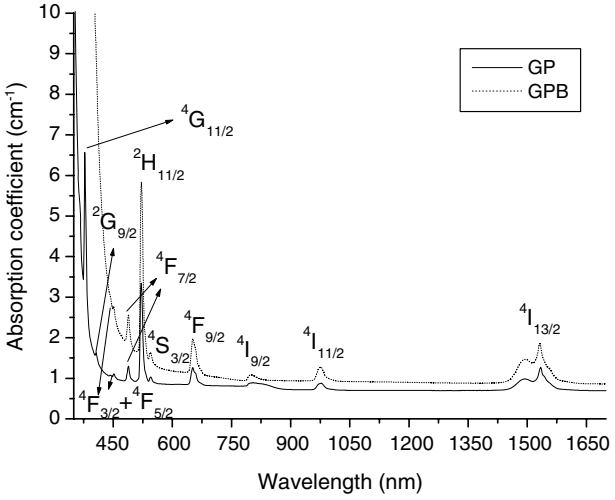


Fig. 1. Absorption coefficient as a function of wavelength for GP and GPB glass fibers, doped with 1.0 wt% of $Er_2O_3$. The electronic transitions from the ground absorption state ($^4I_{15/2}$) to the excited states are presented.

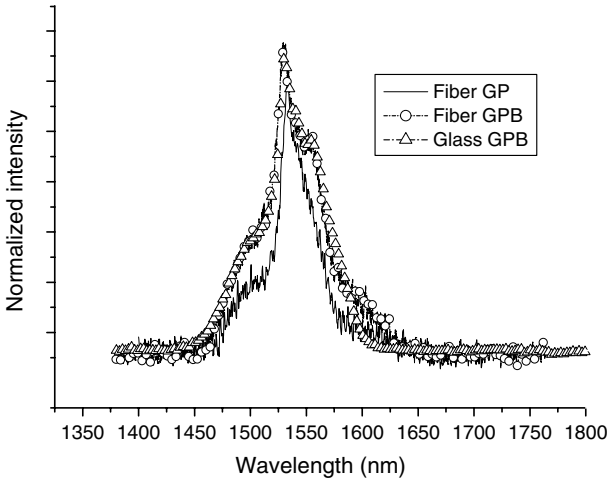


Fig. 2. Emission spectra related to the $^4I_{13/2} \rightarrow {}^4I_{15/2}$ transition for GPB and GP glass fibers. The spectrum of the GPB glass is shown for comparison.

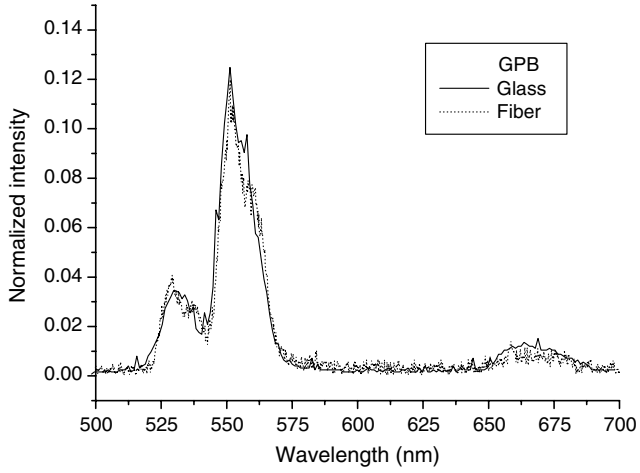


Fig. 3. Upconverted emission spectrum for GPB glass fiber. The spectrum of the glass is displayed for comparison.

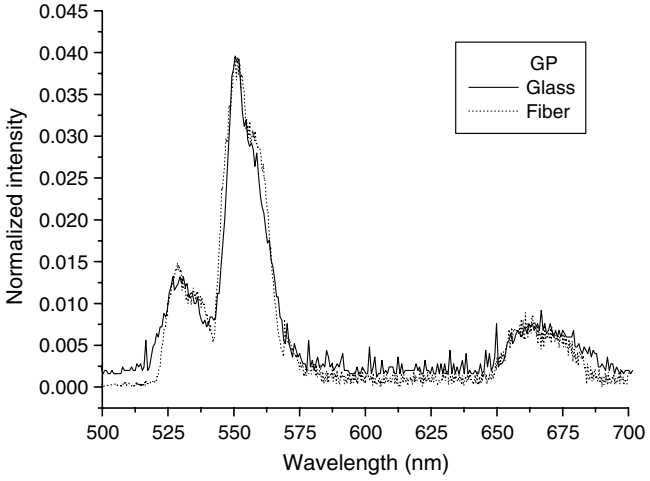


Fig. 4. Upconverted emission spectrum for GP glass fiber. The spectrum of the glass is displayed for comparison.

## 4. Discussion

The mechanism responsible for the emissions in the visible region, which was also observed for the GPB glass [13], is indicated in Fig. 5. It describes the upconversion mechanism based on excited state absorption, in which one pump photon is absorbed and induces the transition $^4I_{15/2} \rightarrow {}^4I_{11/2}$, then a second pump photon promotes the transition $^4I_{11/2} \rightarrow {}^4F_{7/2}$ (solid upwards arrows in Fig. 5). The population, at excited state $^4F_{7/2}$, decays non-radiatively by multiphonon emission (dotted downwards arrow in Fig. 5) to the excited states $^2H_{11/2}$, $^4S_{3/2}$ and $^4F_{9/2}$. These levels emit upconverted photons that originate the emissions shown in Figs. 3 and 4 at 530, 550 and 668 nm (solid downwards arrows in Fig. 5). The pump power dependence of the emission $^4S_{3/2} \rightarrow {}^4I_{15/2}$ was measured for GPB glass [13] and it was confirmed that two photons are required to populate the excited state $^4F_{7/2}$. The same results obtained for GP glass lead the group to the same conclusion. By means of the Raman measurements (Fig. 6), it was possible to confirm the radiative decay from $^4F_{3/2}$ level to $^4I_{15/2}$ ground state (related to the 485 nm emission) because of the presence of the band around 1250 $cm^{-1}$, as will be explained below.

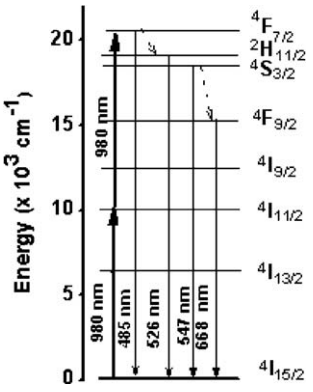


Fig. 5. Energy level diagram and the mechanism of infrared to visible upconversion for $Er^{3+}$-doped GP and GPB glasses, under 980 nm excitation. The lines with arrows denote possible transitions: solid lines represent absorption or emission and dotted lines non-radiative decay by multiphonon emission.

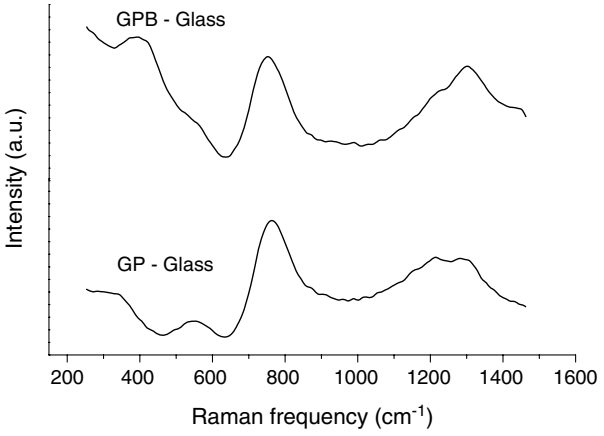


Fig. 6. Raman spectra for GP and GPB glasses doped with 1.0 wt% of $Er_2O_3$.

Comparing Figs. 3 and 4, it can be observed that the efficiency is similar for the upconverted green emissions. However, the intensity of the emission around 668 nm is higher for GP and may be attributed to a short-distance structural relation.

The fluorescence peak positions related to the $^4I_{13/2} \rightarrow {}^4I_{15/2}$ transition (peaked at 1.53 μm and shown in Fig. 2) do not change with glass composition. However, the effective linewidths are different: the effective linewidth decreases as the lead content increases, as reported in previous literature [14]. This explains the difference between the spectra of the fibers, as GP composition has much more lead content than GPB. A structural relation with Pb concentration is indicated by the decrease in the Judd-Ofelt parameter ($\Omega_6$) with the increase in the lead content, already reported for $GeO_2$–PbO and $GeO_2$–PbO–$Bi_2O_3$ glasses [13,14]. The same was also observed in other oxide glasses, such as lead silicates, lead phosphtaes and lead zinc borates [15,16]. The values of $\Omega_6$ are affected more by the amount of $Pb^{2+}$ ions than by the nature of the glass.

Raman spectra are shown in Fig. 6 for GP and GPB glasses. The band around 550 $cm^{-1}$ in germanate glasses is attributed to the deformation of vibrational modes of the glass network structure with bridged anion (i.e. bridged Ge–O–Ge) [8,9]. This band is present in the Raman spectrum of the GP glass. For the GPB glass, only a shoulder around 550 $cm^{-1}$ and a band around 400 $cm^{-1}$, assigned to Bi–O–Bi stretching vibration [9], was observed. It must be stated that there was a relatively high concentration of bismuth oxide in this GPB glass.

At higher frequencies (>600 $cm^{-1}$) a band around 760 $cm^{-1}$, for GP and GPB glasses was observed, due to the stretching vibrational modes of the glass network former. Pure $GeO_2$ glass has phonon bands around 860 $cm^{-1}$. The presence of lead oxide in GP and GPB glasses makes the Ge–O bond weaker, shifting its band to 760 $cm^{-1}$ [8]. Similar Raman spectra were measured for other germanate glasses reported in previous literature [8,9]. The position of the band around 760 $cm^{-1}$ is important because the multiphonon decay of rare-earth ions in a glass depends on this value in the host glass [17,18]. This position did not change for the two different compositions.

The band with a peak around 1250 $cm^{-1}$, as mentioned above, is attributed to $Er^{3+}$ fluorescence ($^4F_{3/2} \rightarrow {}^4I_{15/2}$ transition) at 485 nm. This conclusion is reached by considering the difference between the energies of the incident and scattered radiation, as follows: by considering the laser used for the excitation of the samples in the Raman measurements, 457 nm, which corresponds to 21 882 $cm^{-1}$, and the band of 1250 $cm^{-1}$ from the Raman spectrum; the difference between them is 20 632 $cm^{-1}$, or 485 nm.

No sharp peaks were observed in the Raman measurements, indicating the absence of crystallization. This was

confirmed by the measurement of visible emission spectra of $Er^{3+}$ in the fiber and in the preform, after excitation of 980 nm.

## 5. Conclusions

In this paper, results concerning the upconversion effect on $GeO_2$–PbO–$Bi_2O_3$ and $GeO_2$–PbO glasses and glass fibers doped with $Er^{3+}$ was presented for the first time. The glassy state of the fibers was confirmed by observation of the identical fluorescence signals in the visible and infrared regions. The dominant emission in the visible region is associated to the $^4S_{3/2} \rightarrow {}^4I_{15/2}$ transition of $Er^{3+}$. The visible emissions of the fibers were identified by the infrared to visible upconversion mechanism based on excited state absorption. The results indicate that these glass fibers are good candidates for applications in upconversion fiber optical devices.

## Acknowledgements

We would like to thank CNPq and FAPESP for their support, and Professor G. Maciel for the emission measurements of the glasses at Universidade Federal de Pernambuco. We also thank Professor D. L. A de Faria for carrying out the Raman measurements at Instituto de Química da USP and for the important discussions related to the Raman spectra.

## References

[1] J. Porque, S. Jiang, B. Hwang, et al., SPIE 3942 (2000) 60.
[2] Z. Pan, S.H. Morgan, J. Lumin. 75 (1997) 301.
[3] J. Wang, J.R. Lincoln, W.S. Brocklesby, et al., J. Appl. Phys. 73 (1993) 8066.
[4] D. Lezal, J. Pedlíková, P. Kostka, J. Bludska, M. Poulain, J. Zavadil, J.Non-Cryst. Solids 284 (2001) 288.
[5] D. Lezal, J. Pedlíková, J. Horák, J. Non-Cryst. Solids 196 (1996) 178.
[6] A. Willey, R. Rox Anderson, J.L. Azpiazy, A.D. Bakuus, et al., Laser. Surg. Med. 38 (2006) 1.
[7] R. Balda, A.J. Garcia Adeva, J. Fernández, J.M. Fdez-Navarro, J. Opt. Soc. Am. B 21 (2004) 744.
[8] Z. Pan, S.H. Morgan, A. Loper, V. King, B.H. Long, W.E. Collins, J. Appl. Phys. 77 (9) (1995) 4688.
[9] Z. Pan, S.H. Morgan, K. Dyer, A. Ueda, J. Appl. Phys. 79 (12) (1996) 8906.
[10] Y.G. Choi, J. Heo, J. Non-Cryst. Solids 217 (1997) 199.
[11] M. Wachtler, A. Speghini, S. Pigorini, R. Rolli, J. Non-Cryst. Solids 217 (1997) 111.
[12] R. Balda, J. Férnandez, M. Sanz, A. de Pablos, J.M. Fdez-Navarro, J. Mugnier, Phys. Rev. B 61 (2000) 3384.
[13] L.R.P. Kassab, A.de O. Preto, W. Lozano, F.X. de Sá, G.S. Maciel, J. Non-Cryst. Solids 43–45 (2005) 3468.
[14] M. Wachtler, A. Speghini, K. Gatterer, H.R. Fritzer, D. Ajò, M. Bettinelli, J. Am. Ceram. Soc. 81 (1998) 2045.
[15] J.A. Capobianco, G. Prevost, P.P. Proulx, P. Kabro, M. Bettineli, Opt. Mater. 6 (1996) 175.
[16] G. Ingletto, M. Bettineli, L. Di Sipio, F. Negrisolo, C. Aschieri, Inorg. Chim. Acta 188 (1991) 201.
[17] K. Huang, Contemp. Phys. 22 (1981) 599.
[18] C.B. Layne, W.H. Lowdermilk, M.J. Weber, Phys. Rev. B 16 (1977) 10.